Article

Not peer-reviewed version

Electrochemical Synthesis of Functionalized Graphene/Polyaniline Composite Using Two Electrode Configuration for Supercapacitors

Dong Sheng Yu *, Jili Li *, Tiekun Jia, Binbin Dong, Zhixiao Han, Wenjie Tian, Ruilin Jiang, Xi Lu, Lekang Li, Nam Hoon Kim *, Joong Hee Lee *

Posted Date: 9 November 2023

doi: 10.20944/preprints202311.0610.v1

Keywords: aryl diazonium salt-functionalized graphene (ADS-G); ADS-G/PANI composites; electrochemical polymerization; supercapacitor

Article

Electrochemical Synthesis of Functionalized Graphene/Polyaniline Composite Using Two Electrode Configuration for Supercapacitors

Dong Sheng Yu [1,*], Jili Li [1,*], Tiekun Jia [1], Binbin Dong [1], Zhixiao Han [1], Wenjie Tian [1], Ruilin Jiang [1], Xi Lu [1], Lekang Li [1], Nam Hoon Kim [2,*] and Joong Hee Lee [2,*]

[1] Material Science and Engineering School, Henan Province International Joint Laboratory of Materials for Solar Energy Conversion and Lithium Sodium based Battery & Henan Key Laboratory of Special Protective Materials, Luoyang Institute of Science and Technology, Luoyang 471023, China; tiekun_jia@lit.edu.cn (T.K.J.); dongbb@lit.edu.cn (B.B.D.); zhixiaohan2023@163.com (Z.X.H.); tianwenjie0305@163.com (T.W.J.); jiang_ruilin@163.com (R.L.J.); luxi20031101@163.com (X.L.); lekangli2003@163.com (L.K.L.)

[2] Department of Nano Convergence Engineering, Jeonbuk National University, Jeonju, Jeonbuk 54896, Republic of Korea;

* Correspondence: dongsh_yu@163.com (D.S.Y.); lijili328@126.com (J.L.); nhk@jbnu.ac.kr (N.H.K.); jhl@jbnu.ac.kr (J.H.L.); Tel.: +86-(37)-965928195 (D.S.Y.)

Abstract: An effective approach to fabricate large-scale of conducting polyaniline (PANI) by an in situ anodic electrochemical polymerization on the nickel foam, which coated by a novel aryl diazonium salt (ADS)-functionalized graphene (ADS-G). In present work, ADS-G was used as a high surface area support material for electrochemical polymerization of PANI. Electrochemical performances of the ADS-G/PANI composites exhibited better suitability as supercapacitor electrode materials than that of the PANI. The ADS-G/PANI composites achieved the specific capacitance of 528 F g^{-1}, which was higher than that of PANI (266 F g^{-1}) due to the excellent electrode-electrolyte interaction and synergistic effect of electrical conductivity between ADS-G and PANI in the composites. These findings suggested that the ADS-G/PANI composites were a suitable composite for the potential supercapacitor applications.

Keywords: aryl diazonium salt-functionalized graphene (ADS-G); ADS-G/PANI composites; electrochemical polymerization; supercapacitor

1. Introduction

Since the graphene in its true sense was firstly fabricated in 2004 [1], which shows a flat single layer of carbon atoms tightly packed into a two-dimensional honeycomb lattice [2–5], it is an attractive substrate material in compounding with polymer for the new energy storage like supercapacitor due to its high conductivity and large surface area [6]. On the other hand, conducting polymers (CPs) such as polyaniline (PANI), polypyrrole (PPy), polythiophene (PT) also have been widely explored for supercapacitor in the scientific community [7–9], which provide the conductive through a conjugated bond system along the polymer backbone [10]. Since the high flexibility and relatively high specific capacitance, the CPs are pondered as one of the major electrode materials for supercapacitor applications. The combination of CPs with graphene is expected that can engender some fascinating properties in view of the fascinating effects and the CPs are normally produced into nanostructure to improve the electrochemical performance [11]. Yan et al. synthesized a graphene nanosheets (GNS)/PANI composites using in situ polymerization [12]. Another effective approach for preparation of PPy/graphene nanocomposites were used graphite oxide and pyrrole monomer via in-situ polymerization and subsequently reduced by hydrazine monohydrate [13]. Shi et al. reported that the sulfonated PANI (SPANI) functionalized graphene was stably dispersed in water with enhancement of electrochemical stability and electrocatalytic activity [14]. However, the simple and effective approaches to fabricate the graphene/CPs composites persist scientifically challenging.

 doi:10.20944/preprints202311.0610.v1

PANI is a representative conducting polymer for supercapacitors investigation because of its easy synthesis, good environmental stability, doping/dedoping chemisitry, high conductivity and excellent capacity for energy storage [7,15–17]. However, PANI is impressionable to rapidly reduce the performance of specific capacitance during the repetitive cycles due to its swelling and shrinkage [18]. In order to ease this impediment, the incorporation of carbon based materials in the PANI has been found to enhance the stability and the specific capacitance value at the same time. Recently, graphene/PANI composites with remarkably enhanced performance in supercapacitor electrode materials have been widely investigated due to their conductivity, high surface area and the stability for the energy storage [6]. Cheng et al. prepared the freestanding and flexible graphene/PANI composite paper via an in situ anodic electropolymerization of PANI film on graphene paper with a stable large electrochemical capacitance of 233 F g^{-1} [19]. A hybrid electrode of graphene/PANI composites with an electric double-layer capacitor of graphene nanosheets and a pseudocapacitor of PANI exhibits a synergistic effect with excellent specific capacitance (375.2 F g^{-1}) for flexible thin film supercapacitors [20]. However, the specific capacitance in graphene/PANI composites is less provided by the graphene sheets due to its agglomerated layer-like structure and is mainly dominated from the PANI films coated on the graphene sheets [21]. Therefore, it is important investigation of the electrical and electrochemical properties of functionalized graphene to prevent the reaggregate [22–25].

In the previous study, the functionalized graphene (ADS-G) with stable dispersion in polar solvents and significantly greater electrical conductivity was successfully synthesized using ADS via electrophilic surface modification techniques [26]. In the present work, the ADS-G solution was deposited on one nickel foam (the deposited area is about 1 cm × 1 cm) to prepare the functinalized electrode and followed the electrochemical polymerization of aniline to form the funcitionalized graphene/PANI composites. The electrochemical performances of ADS-G/PANI composites have been studied for further comparison in this article.

2. Experimental

2.1. Materials

Natural graphite flakes were purchased from Sigma-Aldrich (Steinheim, Germany). Aniline was supported from TCI (C_6H_7N, ≥ 98%, Tokyo, Japan). p-toluene sulfonic acid (PTS) was used as the electrolyte for electrochemical polymerization of aniline (Junsei Chemical Co. Ltd, Tokyo, Japan). Sodium 4-aminoazobenzene-4'-sulfonate (TCI, Tokyo, Japan) was used as a pristine agent to synthesize the surface modifier, ADS. Sodium borohydride and hydrazine monohydrate (TCI, Tokyo, Japan) were used as reducing agents, and potassium permanganate (Junsei Chemical Co. Ltd, Tokyo, Japan) was used as oxidizing agent. Sulfuric acid, hydrochloric acid, hydrogen peroxide, and sodium carbonate (Pyeong-taek-si, Samchun Pure Chemical Co. Ltd, Korea) were used as received.

2.2. Synthesis of graphene xodie and ADS-G

Natural graphite flake was used to prepare graphite oxide by a modified Hummers method [26–28]. In an ice bath, approximately 2 g of natural flake graphite was put into 46 mL concentrated sulfuric acid in a 500 mL round bottom flask. The 6 g of $KMnO_4$ powder was added slowly and kept stirring for 2 h in the ice bath. After 2h, the resulting mixture was continued to stir for approximately 6 h at room temperature and then diluted with approximately 100 mL of distilled water and stirred for another 2 h. Subsequently, 5% H_2O_2 solution was added dropwise to remove excess $KMnO_4$ until getting the brilliant yellow colour. The resulting graphite oxide solution was washed with HCl solution and distilled water repeatedly until the pH was approximately 7. The single layer of graphene oxide (GO) was obtained from the resulting graphite oxide by sonication for 30 min in a water bath sonicator, and subsequently by centrifugation to remove the un-exfoliated graphite oxide. The purified GO was freeze-dried (IlShin Lab Co, Ltd, Korea, model FD5505). The resulting GO was dispersed into distilled water and sonicated for 15-20 min to obtain homogeneous dispersion (1 mg mL^{-1}).

 doi:10.20944/preprints202311.0610.v1

The ADS-G was synthesized in three steps according to previous research [26]. Briefly, 100 mg of GO was dispersed in 100 mL distilled water and to this dispersion approximately 800 mg of $NaNH_4$ was added. The pH of this solution was adjusted to 9-10 using a Na_2CO_3 solution and then stirred at 80 °C for 1 h. The resulting mixture was then centrifuged and washed with distilled water several times and then was re-dispersed in 100 mL distilled water. The ADS was prepared from the reaction of 1.2 g of SAS in 5.5 mL of HCl and 11 mL of distilled water with 0.32 g of $NaNO_2$ in an ice bath at approximately 0 °C for 1.5 hours. The ADS solution was then slowly poured into the dispersion of partially-reduced GO with constant stirring for 2 h in the ice bath. Subsequently, 0.05 mL hydrazine monohydrate was added to the dispersion and the reaction mixture was reacted at 100 °C for 12 h with stirring. Finally, the ADS-G was received after washing with distilled water thoroughly and then drying under a vacuum at 60 °C for several days. The resulting ADS-G was finally dispersed in distilled water and formed the dispersion (1 mg mL^{-1}) after sonication for 10-15 min.

2.3. Preparation of ADS-G coated working electrode

Prior to the deposition of ADS-G dispersion, the nickel foam was pretreated as etching in 0.1 M HCl solution for 15 min and sonication in acetone and distilled water for 20 min, respectively. The working electrodes were prepared by mixing 1 mL of the obtained ADS-G solution (1 mg mL^{-1}), powder with 5 wt.% carbon black and 10 wt.% poly(vinyldiene fluoride) (PVDF) binder. A small amount of ethanol was added to the mixture and subsequently sonicated for 30 min to achieve the homogeneous dispersion. The resulted dispersion was coated onto the pretreated nickel foam substrate for the area of 1 × 1 cm^2. The amount of composites onto the resulted working electrode including ADS-G, conducting agent (black carbon) and binder (PVDF) was approximately 1.2 mg.

2.4. Preparation of ADS-G/PANI composites

Aniline was freshly distilled under reduced pressure before use. The area of prepared working electrode was used as anodic electrode for electrochemical polymerization of PANI and the coating area was approximately 1 × 1 cm^2 for composites. A copper foil (1 × 2 cm^2) was used as the counter electrode (cathodic electrode). An auto range DC power supply (IT 6721) was supported the power source. The electrochemical polymerization of aniline was executed in the presence of 0.1 M aniline/0.5 M PTS electrolyte solution. The homogeneous mixture of aniline and PTS solution was obtained after sonication for 30 min. The aniline was electrochemical polymerized on the working electrode at a constant potential (2 V) for 30 min. Subsequently, the working electrode with ADS-G/PANI composites was immersed in 0.5 M H_2SO_4 solution statically to remove the aniline monomer and oligomer PANI from the polymeric film and washed with distilled water and ethanol for several times. The resulting electrode was dried at 60°C in a vacuum for one day. Figure 1 shows the two electrode configuration for the fabrication of ADS-G/PANI composites. For the comparison, PANI was prepared by the same condition as the ADS-G/PANI composites.

Preprints (www.preprints.org) | NOT PEER-REVIEWED | Posted: 9 November 2023 doi:10.20944/preprints202311.0610.v1

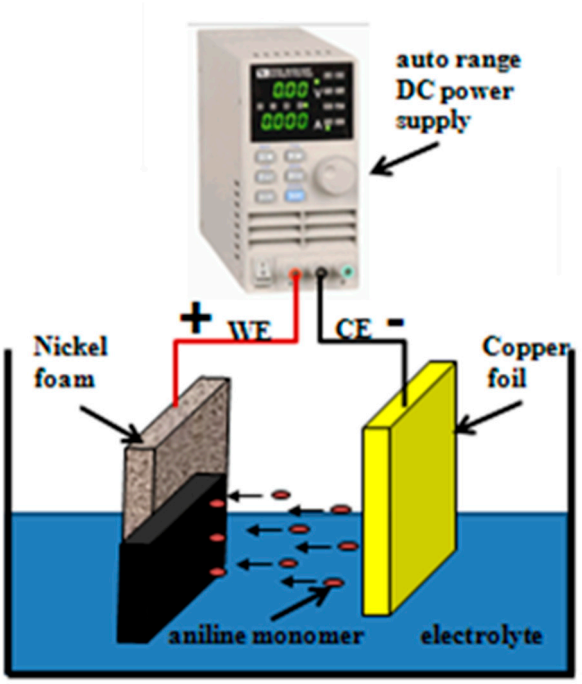

Figure 1. two electrode configuration for the fabrication of ADS-G/PANI composites.

2.5. Characterizations

To observe the fourier transform infrared spectroscopy (FT-IR) analyses, X-ray diffraction (XRD) patterns, the morphology through a field emission scanning electron microscopy (FE-SEM), and the thermogravimetric analyses (TGA) of the ADS-G, PANI, and ADS-G/PANI composites precisely, the nickel foam was etching away by a hot HCl or FeCl3 solution and then washed by distilled water prior to the measurement. The FT-IR analyses of the ADS-G, PANI, and ADS-G/PANI composites powder samples that were mixed with KBr and pressed into thin pellets were performed with a Nicolet 6700 spectrometer (Thermo Scientific, USA) over a wavenumber range of 4000-400 cm^{-1}. The XRD patterns of ADS-G, PANI, and ADS-G/PANI composites were executed at room temperature on a D/Max 2500V/PC (Rigaku Corporation, Tokyo, Japan) using a Cu target (λ=0.154 nm) with the scan rate of 2° (2θ) min^{-1}, and the range of 5-60°. The morphology of ADS-G, PANI, and ADS-G/PANI composites after etching away the nickel foam and energy-dispersive X-ray spectroscopy (EDS) elemental mapping of ADS-G were observed on a FE-SEM (JSM-6701F, JEOL, Japan). The TGA of ADS-G, PANI, and ADS-G/PANI composites were carried out by a Q50 TG analyzer (TA Instruments, New Castle, DE, USA) from room temperature to 800 °C at a linear heating rate of 5 °C min^{-1} in a nitrogen atmosphere. Electrochemical performances of ADS-G, PANI, and ADS-G/PANI composites electrodes were studied using CH660D electrochemical workstation. The cyclic voltammograms (CV), and charge/discharge characteristics were carried out in a three electrode apparatus: a platinum foil electrode serving as the counter electrode, a saturated Ag/AgCl, Cl^- electrode as the reference electrode and 6M KOH solution as the electrolyte for all electrochemical measurements.

3. Results and discussion

3.1. FT-IR spectra analysis

The FT-IR spectra were used to characterize ADS-G, PANI, and ADS-G/PANI composites. Figure 2 shows the asymmetric and symmetric stretching vibrations of S-O and O=S=O groups of $-SO_3^-$ appeared at ~698 and 1260 cm^{-1}, respectively. The new peaks of the sulfonic acid group and the C-H out-of-plane vibrations of the benzene ring of ADS molecules were observed at ~1026 and ~804 cm^{-1} [26]. For the PANI powder sample, the absorption peaks appeared at 1563 and 1484 cm^{-1},

Preprints (www.preprints.org) | NOT PEER-REVIEWED | Posted: 9 November 2023 doi:10.20944/preprints202311.0610.v1

corresponding to quinoid ring and benzenoid rings in the emeraldine salt, respectively [29]. The appearance of two peaks at 1295 and 1124 cm^{-1} were ascribed to the C-N stretching of the secondary aromatic amine and aromatic C-H bending in the plane [30]. In the case of ADS-G/PANI composites, both of the characteristic peaks of the ADS-G and the PANI were observed in the ADS-G/PANI composites. These findings suggested that the ADS-G/PANI composite was successfully synthesized by method of the electrochemical polymerization.

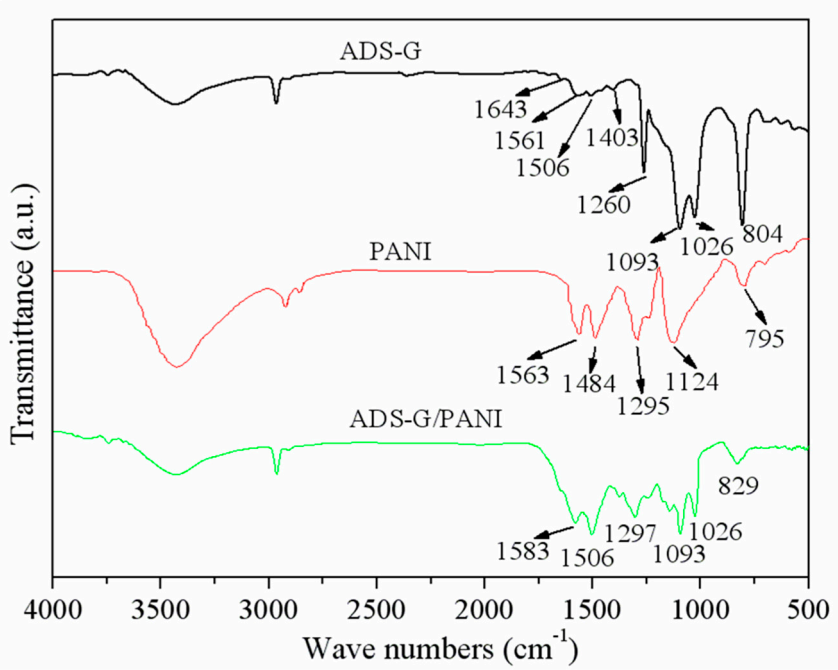

Figure 2. FT-IR spectra of ADS-G, PANI, and ADS-G/PANI composites.

3.2. XRD

Figure 3 shows the XRD patterns of GO, ADS-G, PANI, and ADS-G/PANI composites. The representative diffraction peak of GO was observed at approximately 2θ =10.2°, and the basal reflection (002) peak at 2θ =26.5°of pristine graphite disappeared in GO [31,32], corresponding to the increased interplaner spacing of GO sheets due to the intercalation of the new oxygen-containing functional groups and water molecules between the graphite layers [33]. In the case of ADS-G, a very weak peak at 2θ =23.5° in the ADS-G was observed because of the formation of few agglomerated sheets of graphene and the peak at 2θ =10.2° disappeared, certifying the reduction of GO, long range disorder in graphene, and complete exfoliation of GO [34]. For PANI specimens, the characteristic peaks appeared at 2θ = 9.4°, 15.1°, 20.5°, and 25.2°, corresponding to (001), (011), (020), and (200) refections of in its emeraldine salt form, respectively [35]. The XRD of the ADS-G/PANI composite exhibited much broader at 2θ = 25.2° and weaker at 2θ = 9.4°, 15.1° and 20.5° than that of PANI, indicating that no additional crystalline order was introduced into the ADS-G/PANI composite and ADS-G was interacted with PANI particles.

 doi:10.20944/preprints202311.0610.v1

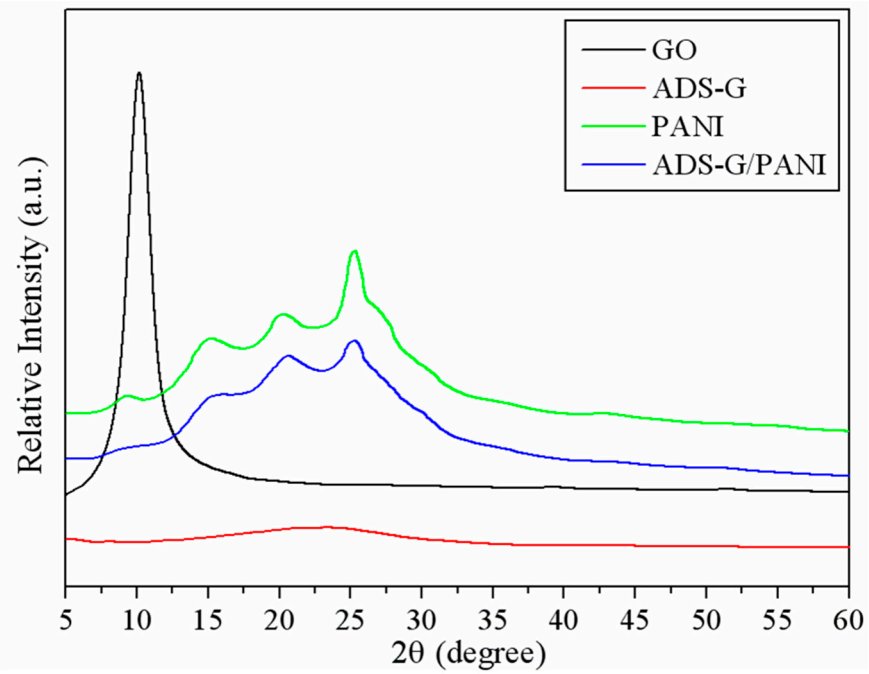

Figure 3. XRD patterns of GO, ADS-G, PANI, and ADS-G/PANI composites.

3.3. FE-SEM analysis

The morphologies of the prepared ADS-G, PANI, and ADS-G/PANI composites were observed by FE-SEM. Figure 4 shows the FE-SEM images of ADS-G, PANI, ADS-G/PANI composites, and EDS of ADS-G respectively. Figure 4a and 4b exhibited the thin wrinkled flakes suggesting high surface area of ADS-G after etching away from nickel foam electrode. From the EDS analysis (Figure 4c), the characteristic peaks for nitrogen and sulfur were clearly found, and typical peaks for nickel weren't observed in the ADS-G sheets, respectively. This result indicated the ADS-G sheets were fully etched away from the nickel foam. During electrochemical polymerization of PANI without ADS-G supported material, PANI displayed worm-like morphology with a diameter about 100-150 nm and a length with 1-2 μm which was stacked by spherical particles in Figure 4d and 4e. Compare to the morphologies of the ADS-G and PANI, Figure 4f and 4g showed obviously different morphologies of ADS-G/PANI composites. In the images, the PANI particles grew on the surfaces of ADS-G, which was like a support material that could provide a large number of active sites for nucleation of PANI [36–38]. This morphology of ADS-G/PANI composites could increase both the dispersion of PANI and the contact of PANI with electrolyte, and therefore may be enhanced the electrochemical performance as an electrode for surpercapacitor [36].

Preprints (www.preprints.org) | NOT PEER-REVIEWED | Posted: 9 November 2023 doi:10.20944/preprints202311.0610.v1

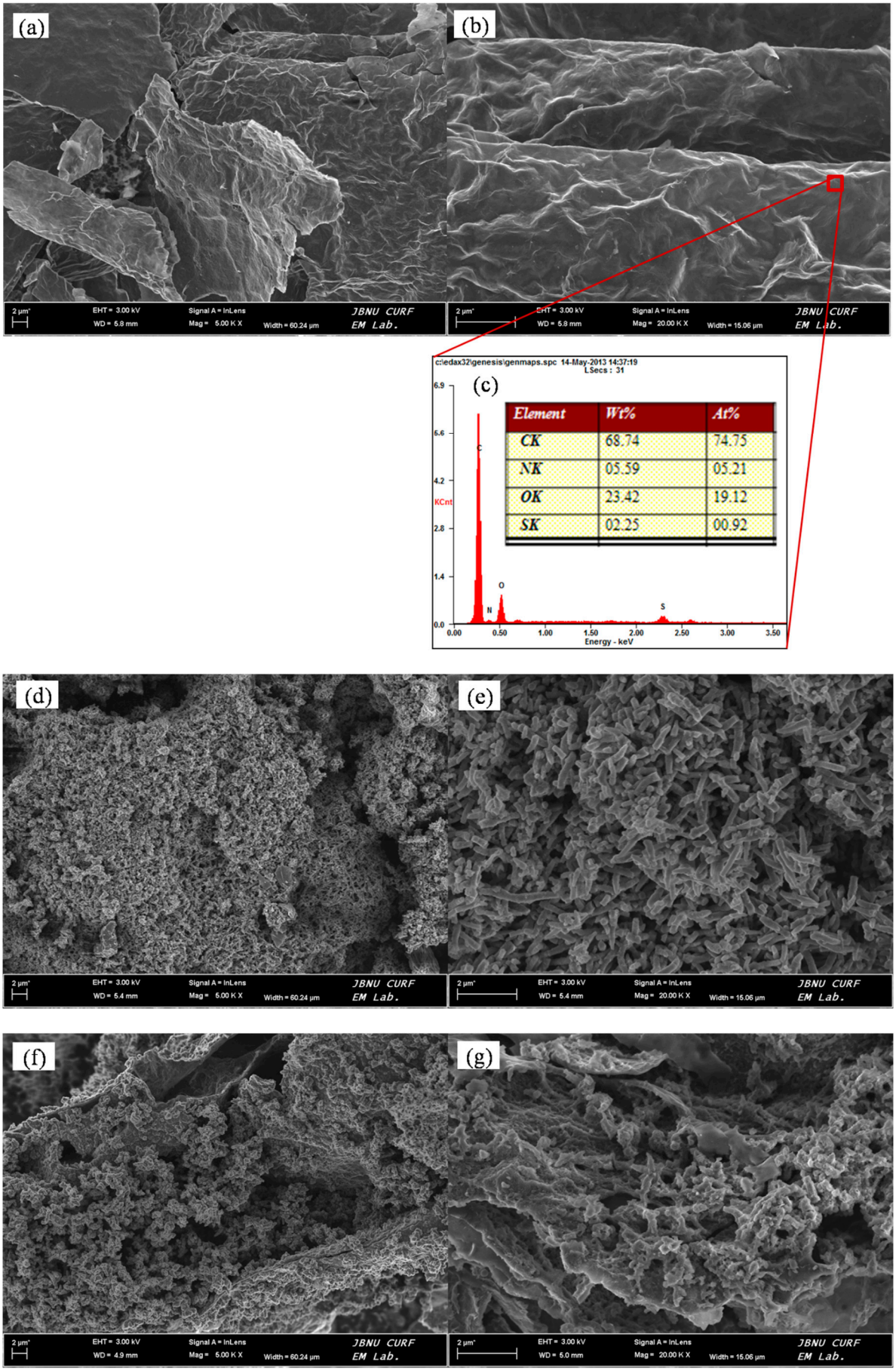

Figure 4. FESEM images of ADS-G (a, b), PANI (d, e), ADS-G/PANI composites (f, g) and EDS of ADS-G (c); (a, d, f) Low-magnification of 5,000 and (b, e, g) High-magnification of 20,000.

 doi:10.20944/preprints202311.0610.v1

3.4. TGA

The TGA of ADS-G, PANI, and ADS-G/PANI composites were shown in Figure 5. The significant mass loss of ADS-G was approximately at 220 °C due to the thermal decomposition process of $PhSO_3H$ group and elimination of residual oxygen functionalities on the surface of ADS-G [26]. The as-prepared PANI was thermally unstable and showed slight mass loss below 150 °C due to the absorbed moisture in PANI particles. Subsequently, the PANI exhibited a two step weight loss. The first main mass loss was observed between 150 and 300 °C may be due to the loss dopant, impurities, and monomer. The second major mass loss was approximately 400 °C, corresponding to the degradation of the PANI [39]. However, it can be noted that ADS-G/PANI composites showed enhanced thermal stability as compared to that of PANI, indicating the existence of thermally stable ADS-G. The overall mass losses of PANI and ADS-G/PANI composites at 800 °C were approximately 68.91 and 59.59% respectively, indicating approximately 9.3% ADS-G introduced into ADS-G/PANI composites. The improved thermal stability of ADS-G/PANI composites compared to that of PANI may be attributed to the interaction between ADS-G and PANI chains.

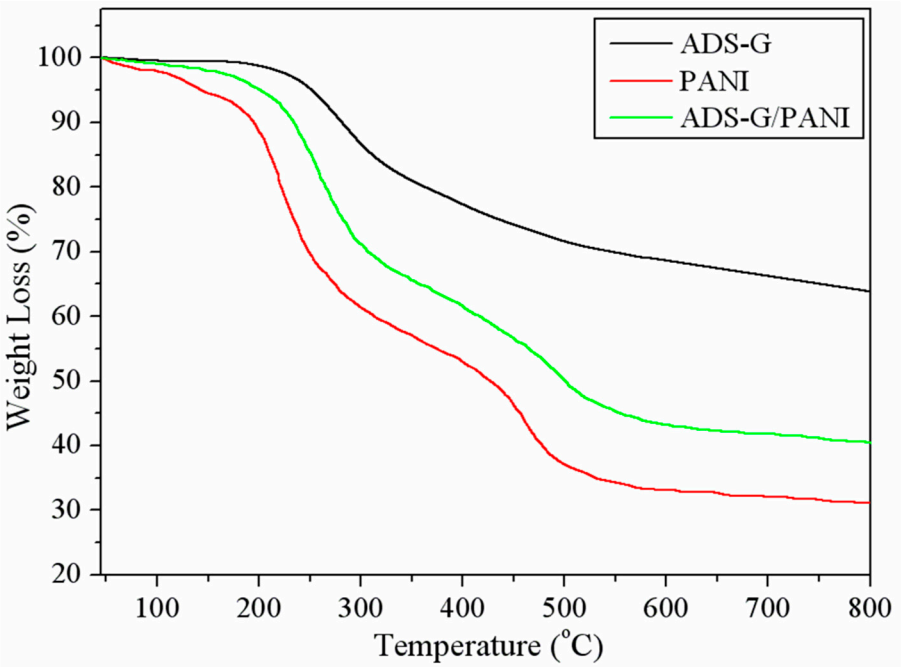

Figure 5. TGA curves of ADS-G, PANI, and ADS-G/PANI composites.

3.5. Electrochemical properties

Figure 6 depicts the CV of PANI and ADS-G/PANI composites at a scan rate of 50 mV s^{-1} in 6M KOH solution. Both the PANI and ADS-G/PANI composites exhibited a couple of redox peaks that are faradic transition of PANI from a leucoemeraldine form (semiconducting state) to emeraldine form (conducting state), which indicated the typical pseudocapacative characteristic of PANI [18]. The area surrounded by the CV curve of ADS-G/PANI composites was apparently larger than that of the PANI at the same scan rate, indicating higher specific capacitance.

Preprints (www.preprints.org) | NOT PEER-REVIEWED | Posted: 9 November 2023 doi:10.20944/preprints202311.0610.v1

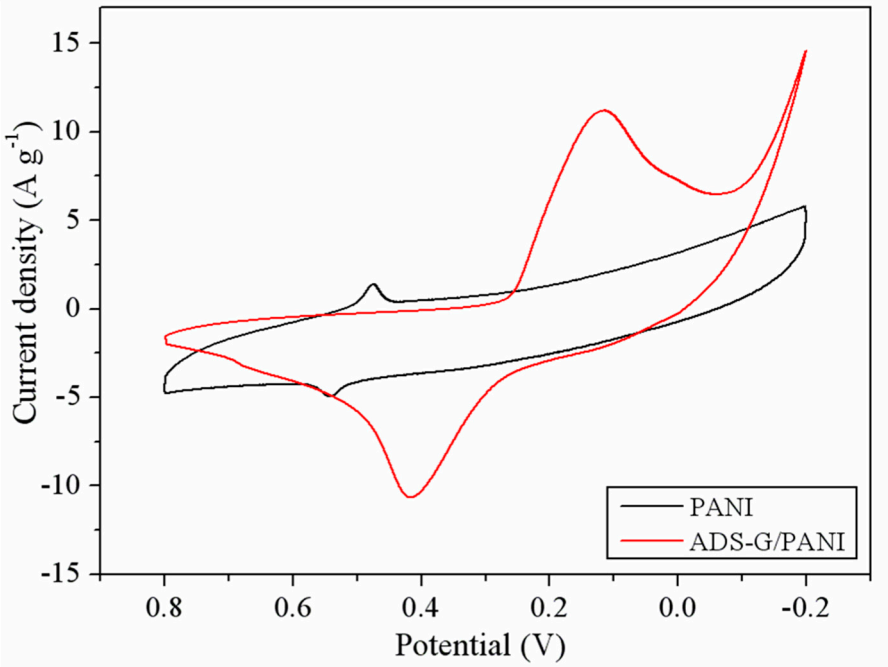

Figure 6. CV curves of PANI and ADS-G PANI composites at a scan rate of 50 mV s^{-1} in 6 M KOH.

Figure 7 shows the CV curves for PANI and ADS-G/PANI composites. The CV curves (Figure 7a) of the PANI exhibited a combination of EDLC and pseudocapacitance behavior. However, shapes of the CV curves ADS-G/PANI showed more pseudocapacitance behavior than the EDLC behavior (Figure 7b). The redox peaks of the PANI and ADS-G/PANI composites are attributed to the faradic transformation of PANI from leucoemeraldine form to emeraldine form. It is also noted that the cathodic peaks (C_1) shifted negatively and the anodic peaks (A_1) shifted positively in both of PANI and ADS-G/PANI composites with the increasing potential scan rates from 10 mV s^{-1} to 200 mV s^{-1}. The area under CV curves of both the PANI and ADS-G/PANI composites became broader and remained undistorted with increasing the scan rate indicating excellent supercapacitor behavior up to high scan rate. And the ADS-G/PANI showed better supercapacitor behavior than that of the PANI, which may be due to the ADS-G coated nickel foam electrode served as the high surface area support material for the polymerization of PANI and ADS-G in the composites also offered highly conductive path [40]. The as-prepared ADS-G/PANI composites could provide enhanced electrode/electrolyte interface areas that can enhance the electrochemical accessibility of electrolyte.

Preprints (www.preprints.org) | NOT PEER-REVIEWED | Posted: 9 November 2023 doi:10.20944/preprints202311.0610.v1

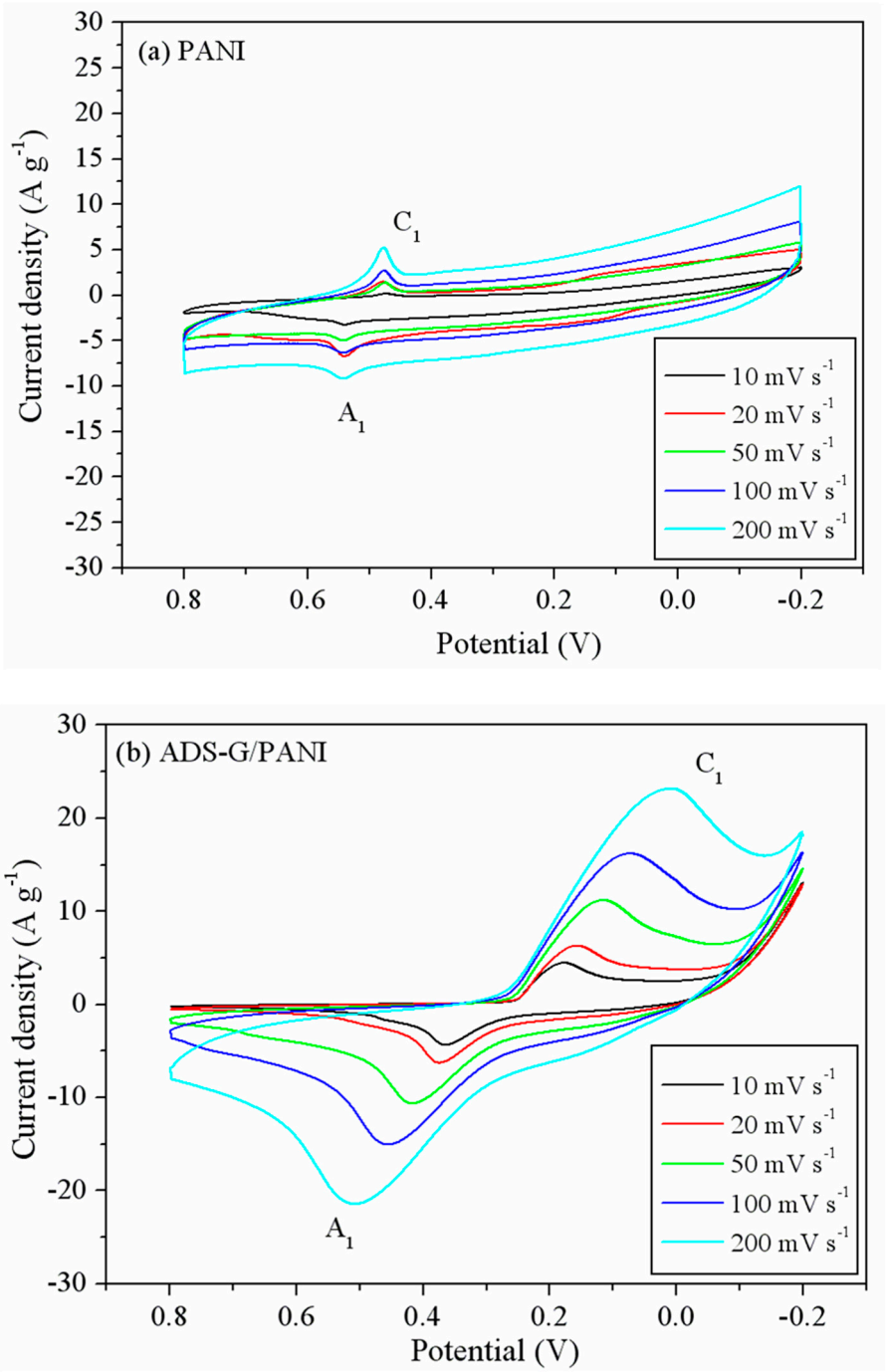

Figure 7. CV curves of (a) PANI and (b) ADS-G/PANI at various scan rates.

In order to evaluate the specific capacitance of PANI and ADS-G/PANI composites, the charge/discharge curves were carried out as shown in Figure 8. The charge/discharge cycles of the PANI and ADS-G/PANI composites electrodes were executed at a constant current density of 1 A g^{-1}. The specific capacitance can be calculated according to equation $C=I\Delta t/(m\Delta V)$, Where, C (F g^{-1}) is the specific capacitance of the materials, I (A) is the applied current, t (s) is the discharge time, V (V) is the applied potential and m (g) is the mass of PANI or ADS-G/PANI composites coated on the nickel electrode. The ADS-G/PANI composites displayed the specific capacitance of 528 F g^{-1} compared to that of 266 F g^{-1} for PANI. The better specific capacitance of ADS-G/PANI composites compared to that of the PANI is due to the excellent electrode-electrolyte interaction and synergistic effect of electrical conductivity between ADS-G and PANI in the composites.

Preprints (www.preprints.org) | NOT PEER-REVIEWED | Posted: 9 November 2023 doi:10.20944/preprints202311.0610.v1

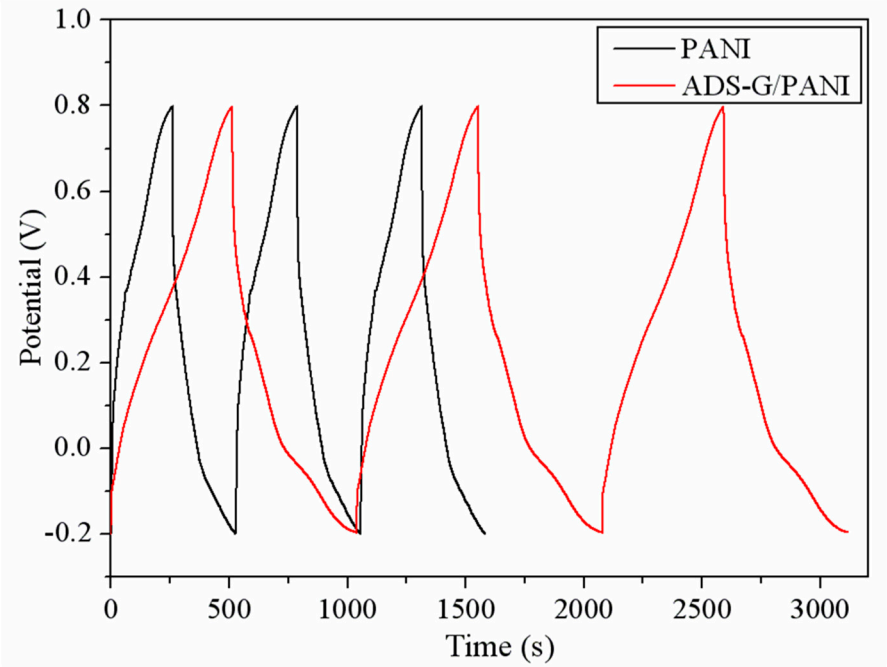

Figure 8. charge-discharge behavior of PANI and ADS-G/PANI composite based supercapacitors performed at a constant current density of 1 A g^{-1}.

Figure 9 performs the cyclic stability of the PANI and the ADS-G/PANI composites. From the image, the ADS-G/PANI composites maintained its 89.4% specific capacitance of the original value after 1000 charge/discharge cycles, which was showed more excellent cyclic stability than that of the PANI (66.3%). The high specific capacitance and good cycling stability of the ADS-G/PANI composites supercapacitor might be resulted from the more perfect coverage structure, the larger specific area, and higher conductivity of the ADS-G/PANI composites compared to that of the PANI.

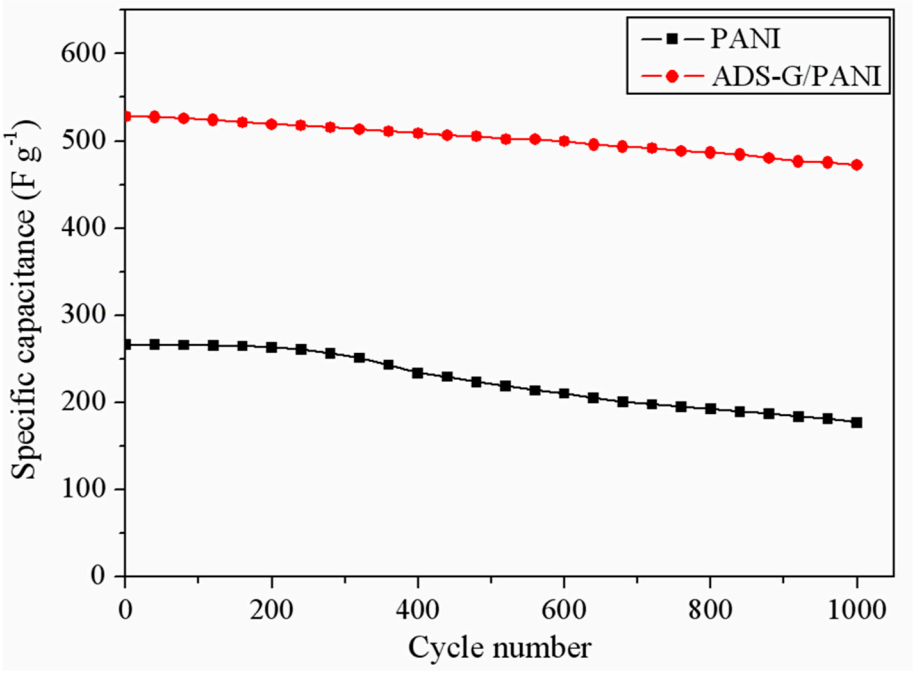

Figure 9. Cycling stability of PANI and ADS-G/PANI composites recorded at 1 A g^{-1}.

4. Conclusions

The ADS-G, which coated on the nickel foam, was further studied as the high surface area support material for electrochemical polymerization of PANI. The PANI particles were successfully grown on the surface of ADS-G sheets as evidence by FT-IR. The morphologies of ADS-G, PANI, and ADS-G/PANI composites after etching away the nickel foam from the electrodes were confirmed by FE-SEM analysis. From the FE-SEM and EDS analyses, the large-area of the ADS-G for the support materials was achieved. TGA suggested the incorporation of ADS-G with PANI was enanhanced the thermal stability compared to that of the PANI. Electrochemical performances of both the ADS-G/PANI composites and PANI were shown their suitability as supercapacitor electrode materials. From the charge/discharge curves, the specific capacitance of ADS-G/PANI composites was about 528 F g^{-1}, which was higher than that of PANI (266 F g^{-1}) due to the excellent electrode-electrolyte interaction and synergistic effect of electrical conductivity between ADS-G and PANI in the composites. These results suggest that the ADS-G/PANI is a suitable composite for the potential supercapacitor applications.

Author Contributions: Conceptualization, D.S.Y.; methodology, J.L. and N.H.K.; Experiments, R.L.J., X.L. and L.K.L.; formal analysis, Z.X.H., T.W.J., R.L.J., X.L. and L.K.L.; investigation, T.K.J. and B.B.D.; resources, J.L. and T.K.J.; writing—original draft preparation, D.S.Y.; writing—review and editing, N.H.K. and J.H.L.; supervision, J.H.L. All authors have read and agreed to the published version of the manuscript.

Funding: This research was funded by National Natural Science Foundation of China (52202064) and Henan Science and Technology Department, China (Henan Science and Technology Research Program, 232102521021 and 222102520005).

Acknowledgments: This study was supported by the Human Resource Training Project for Regional Innovation, the Converging Research Center Program (2012K001428), and the World Class University (WCU) program (R31-20029) through the National Research Foundation (NRF) funded by the Ministry of Education, Science, and Technology (MEST) of Korea.

Conflicts of Interest: The authors declare no conflict of interest.

References

1. Novoselov K.S.; Geim A.K.; Morozov S.V.; Jiang D.; Zhang Y.; Dubonos S.V.; Grigorieva I.V.; Firsov A.A. Electric field effect in atomically thin carbon films. *Science* **2004**, 306(5696), 666-669.
2. Geim A.K.; Novoselov K.S. The rise of graphene. *Nat. Mater.* **2007**, 6, 183-191.
3. Novoselov K.S.; Geim A.K.; Morozov S.V.; Jiang D.; Katsnelson M.I.; Grigorieva I.V.; Dubonos S.V.; Firsov A.A. Two-dimensional gas of massless dirac fermions in graphene. *Nature* **2005**, 438, 197-200.
4. Li D.; Kaner R.B. Graphene-based materials. *Science* **2008**, 320(5880),1170-1171.
5. Bunch J.S.; Zande A.M.V.D.; Verbridge S.S.; Frank L.W.; Tanenbaum D.M.; Parpia J.M.; Craighead H.G.; McEuen P.L. Electromechanical resonators from graphene sheets. *Science* **2007**, 315(5811), 490-493.
6. Choi H.J.; Jung S.M.; Seo J.M.; Chang D.W.; Dai L.M.; Baek J.B. Graphene for energy conversion and storage in fuel cells and supercapacitors. *Nano Energy* **2012**, 1(4),534-551.
7. Ryu K.S.; Kim K.M.; Park N.G.; Park Y.J.; Chang S.H. Symmetric redox supercapacitor with conducting polyaniline electrodes. *J. Power Sources* **2002**, 103(2), 305-309.
8. Faverolle F.; Attias A.J.; Bloch B. Highly conducting and strongly adhering polypyrrole coating layers deposited on glass substrates by a chemical process. *Chem. Mater.* **1998**, 10(3), 740-752.
9. Lota K.; Khomenko V.; Frackowiak E. Capacitance properties of poly(3,4-ethylenedioxythiophene)/carbon nanotubes composites. *J. Phys. Chem. Solids* **2004**, 65(2-3), 295-301.
10. Snook G.A., Kao P., Best A.S. Conducting-polymer-based supercapacitor devices and electrodes. *J. Power Sources* **2011**, 196(1), 1-12.
11. Tang Y.H.; Wu N.; Luo S.L.; Liu C.B.; Wang K.; Chen L.Y. One-step electrodeposition to layer-by-layer graphene-conducting-polymer hybrid films. *Macromol. Rapid Commun.* **2012**, 33(20), 1780-1786.
12. Yan J.; Wei T.; Shao B.; Fan Z.J.; Qian W.Z.; Zhang M.L.; Wei F. Preparation of a graphene nanosheet/polyaniline composite with high specific capacitance. *Carbon* **2010**, 48(2), 487-493.

13. Bose S; Kuila T.; Uddin M.E.; Kim N.H.; Lau A.K.T.; Lee J.H. In-situ synthesis and characterization of electrically conductive polypyrrole/graphene nanocomposites. *Polymer* **2010**, 51(25), 5921-5928.
14. Bai H.; Xu Y.X.; Zhao L.; Li C.; Shi G.Q. Non-covalent functionalization of graphene sheets by sulfonated polyaniline. *Chem. Commun.* **2009**, 13, 1667-1669.
15. Li D.; Huang J.X.; Kaner R.B. Polyaniline nanofibers: a unique polymer nanostructure for versatile applications. *Acc. Chem. Res.* **2009**, 42(1), 135-145.
16. Bai H.; Shi G.Q. Gas sensors based on conducting polymers. *Sensors* **2007**, 7(3), 267-307.
17. Lee R.H.; Lai H.H.; Wang J.J.; Jeng R.J.; Lin J.J. Self-doping effects on the morphology, electrochemical and conductivity properties of self-assembled polyanilines. *Thin Solid Films* **2008**, 517(2), 500-505.
18. Li J.; Xie H.; Li Y.; Liu J.; L Z.X. Electrochemical properties of graphene nanosheets/polyaniline nanofibers composites as electrode for supercapacitors. *J. Power Sources* **2011**, 196(24), 10775-10781.
19. Wang D.W.; Li F.; Zhao J.P.; Ren W.C.; Chen Z.G.; Tan J.; Wu Z.S.; Gentle l.; Lu G.Q.; Cheng H.M. Fabrication of graphene/polyaniline composite paper via in situ anodic electropolymerization for high-performance flexible electrode. *ACS Nano* **2009**, 3(7), 1745-1752.
20. Lee T.M.; Yun T.Y.; Park B.H.; Sharma B.; Song H.K.; Kim B.S. Hybrid multilayer thin film supercapacitor of graphene nanosheets with polyaniline: importance of establishing intimate electronic contact through nanoscale blending. *J. Mater. Chem.* **2012**, 22(39), 21092-21099.
21. Zhang K.; Zhang L.L.; Zhao X.S.; Wu J.S. Graphene/polyaniline nanofiber composites as supercapacitor electrodes. *Chem. Mater.* **2010**, 22 (4), 1392-1401.
22. Si Y.C.; Samulski E.T. Synthesis of water soluble graphene. *Nano Lett.* **2008**, 8(6), 1679-1682.
23. Kuila T.; Khanra P.; Bose S.; Kim N.H.; Ku B.C.; Moon B.H.; Lee .JH. Preparation of water –dispersible graphene by facile surface modification of graphite oxide. *Nanotechnology* **2011**, 22(30), 305710.
24. Li F.H.; Bao Y.; Chai J.; Zhang Q.X.; Han D.X.; Niu L. Synthesis and application of widely soluble graphene sheets. *Langmuir* **2010**, 26(14), 12314-12320.
25. Hao R.; Qian W.; Zhang L.H.; Hou Y.L. Aqueous dispersions of TCNQ-anion-stabilized graphene sheets. *Chem. Commun.* **2008**, 48, 6576-6578.
26. Yu D.S.; Kuila T.; Kim N.H.; Khanra P.; Lee J.H. Effects of covalent surface modifications on the electrical and electrochemical properties of graphene using sodium 4-aminoazobenzene-4'-sulfonate. *Carbon* **2013**, 54, 310-322.
27. Hummers W.S.; Offeman R.E. Preparation of graphitic oxide. *J. Am. Chem. Soc.* **1958**, 80(6), 1339.
28. Kuila T.; Bose S.; Khanra P.; Mishra A.K.; Kim N.H.; Lee J.H. A green approach for the reduction of graphene oxide by wild carrot root. *Carbon* **2012**, 50(3), 914-921.
29. Zhao Y.; Tang G.S.; Yu Z.Z.; Qi J.S. The effect of graphite oxide on the thermoelectric properties of polyaniline. *Carbon* **2012**, 50(8), 3064-3073.
30. Yan X.B.; Chen J.T.; Yang J.; Xue Q.J.; Miele P. Fabrication of free-standing, electrochemically active, and biocompatible graphene oxide−polyaniline and graphene−polyaniline hybrid papers. *ACS. Appl. Mater. Interfaces.* **2010**, 2(9), 2521-2519.
31. Liu X.; Wang X.Y.; He P.Y.; Yi L.H.; Liu Z.L.; Yi X. Influence of borohydride concentration on the synthesized Au/graphene nanocomposites for direct borohydride fuel cell. *J. Solid State Electrochem.* **2012**, 16, 3929-3937.
32. Machado B.F.; Serp P. Graphene-based materials for catalysis. *Catal. Sci. Technol.* **2012**, 2(1), 54-75.
33. Moon I.K.; Lee J.H.; Ruoff R.S.; Lee H.Y. Reduced graphene oxide by chemical graphitization. *Nat. Commun.* **2010**, 1, 73-78.
34. Kaniyoor A.; Baby T.T.; Ramaprabhu S. Graphene synthesis via hydrogen induced low temperature exfoliation of graphite oxide. *J. Mater. Chem.* **2010**, 20(39), 8467-8469.
35. Pouget J.P.; Józefowicz M.E.; Epstein A.J.; Tang X.; MacDiarmid A.G. *Macromolecules* **1991**, 24(3), 779-789.
36. Zhang J.T.; Zhao X.S. Conducting polymers directly coated on reduced graphene oxide sheets as high-performance supercapacitor electrodes. *J. Phys. Chem. C* **2012**, 116(9), 5420-5426.
37. Zhu J.H.; Chen M.J.; Qu H.L.; Zhang X.; Wei H.G.; Luo Z.P.; Colorado H.A.; Wei S.Y.; Guo Z.H. Interfacial polymerized polyaniline/graphite oxide nanocomposites toward electrochemical energy storage. *Polymer*, **2012**, 53(25), 5953-5964.
38. Li J.; Xie H.Q.; Li Y.; Liu J.; Li Z.X. Electrochemical properties of graphene nanosheets/polyaniline nanofibers composites as electrode for supercapacitors. *J. Power Sources* **2011**, 196(24), 10775-10781.

39. Haldorai Y.; Nguyen V.H.; Shim J.J. Synthesis of polyaniline/Q-CdSe composite via ultrasonically assisted dynamic inverse emulsion polymerization. *Colloid Polym. Sci.* **2011**, 289, 849-854.
40. Wang H.L.; Hao Q.L.; Yang X.J.; Lu L.D.; Wang X. Effect of graphene oxide on the properties of its composite with polyaniline. *ACS Appl. Mater. Interfaces.* **2010**, 2(3), 821-828.